

SUB-PICOSECOND X-RAY STREAK CAMERA USING HIGH-GRADIENT RF CAVITIES*

F. Toufexis[†], V.A. Dolgashev, SLAC, Menlo Park, CA 94025

Abstract

We are developing an ultrafast diagnostic system for X-ray beams from Synchrotron Light Sources and Free-Electron Lasers. In this system, the X-ray beam is focused on the photocathode of a high-gradient radio-frequency cavity that accelerates the photo-emitted electrons to a few MeV while preserving their time structure. The accelerated electron beam is streaked by radio-frequency deflectors and then imaged on a screen. This approach will allow orders of magnitude improvement in time resolution over traditional streak cameras and could potentially enable time-resolved diagnostics of sub-100 fs X-ray pulses. We present preliminary beam dynamics simulations of this system and discuss the implementation.

INTRODUCTION

Streak cameras are instruments for measuring the variation in a pulse of light's intensity with time. The time structure of the incident light pulse can be encoded onto an electron beam through a photocathode. The photo-electrons are accelerated and streaked producing a 2D image on a screen, from which the intensity versus time of the initial light pulse can be inferred. Streak cameras have been used in particle accelerators for a variety of instrumentation tasks including bunch length measurements, longitudinal instability measurements, characterization of Free-Electron Laser (FEL) performance, and synchronization in pump-probe experiments [1]. They have also been used for plasma diagnostics [2–4]. The 2D image of visible light streak cameras was used to create a 2D movie of a light pulse [5–7]. The same concept has been studied for an X-ray streak camera [8].

The typical time resolution of X-ray streak cameras is on the order of a few ps, primarily limited by the bunch lengthening due to the initial energy spread of the photo-electrons and low accelerating field on the photocathode. With photocathode fields on the order of 10 kV mm⁻¹, single-shot sub-picosecond streak cameras have been demonstrated with 600 fs Full Width Half Max (FWHM), 350 fs rise time, and 50 fs timing jitter [3, 9–11]. In accumulation mode, time resolution down to 233 fs was achieved [12, 13]. However, these experiments used UV light instead of an X-ray beam. In was shown in simulation that using low-power accelerating RF fields may improve the resolution down to 100 fs [14, 15]. THz radiation [16] and laser light [17, 18] have shown resolution of 10 fs and 100 as, respectively. RF deflectors have been used to capture ultrafast processes in a single shot in Ultrafast Electron Diffraction (UED) [19–21].

In this work we propose the use of a high-gradient RF photo-injector and RF deflector as an ultra-high-resolution X-ray streak camera operating in either single-shot or accumulation mode. We begin by examining the time resolution limits of X-ray streak cameras and show how high gradients can improve the resolution by 1 - 2 orders of magnitude. We further discuss implementation issues and present preliminary beam dynamics simulations of this system with beam dynamics code ASTRA [22].

TIME RESOLUTION LIMITS

The time resolution of streak cameras is limited by several factors including bunch lengthening due to the initial energy spread of the photo-electrons and low accelerating field on the photocathode, the deflection speed, and space charge [3, 9, 23]. These effects can be wrapped into $\Delta t = \sqrt{\Delta t_j^2 + \Delta t_e^2 + \Delta t_a^2 + \Delta t_d^2 + \Delta t_s^2 + \Delta t_{sc}^2}$, where Δt_j is the time jitter for accumulation mode, Δt_e is the time spread of the secondary photo-electrons (typically ignored since it is on the order of 10 fs [24]), Δt_a is the bunch lengthening due to the initial energy spread of the photo-electrons and accelerating field on the photocathode, Δt_d is the bunch lengthening due to the drift between the anode and sweeping plates, Δt_s is the time error due to the finite transverse emittance and the finite deflection speed, and Δt_{sc} is the bunch lengthening due to space charge. The bunch lengthening due to the initial energy spread of the photo-electrons and accelerating field on the photocathode for a constant gradient can be written as [9]

$$\Delta t_a = \frac{2.63\sqrt{\delta E}}{V_a} \text{ (ps)}, \quad (1)$$

where δE is the FWHM of the electron energy in eV, and V_a is the accelerating field on the photocathode in kV mm⁻¹. In traditional streak cameras V_a is on the order of 10 MV m⁻¹.

High-gradient warm S-Band (2.858 GHz) and X-Band (11.424 GHz) photo-injectors can operate at cathode accelerating fields up to 130 MV m⁻¹ and 200 MV m⁻¹, respectively [25]. High-gradient cryogenic copper at 45 K X-Band (11.424 GHz) photo-injectors can operate at surface fields up to 500 MV m⁻¹ [26] – a factor of 50 improvement over state-of-art X-ray streak cameras, reducing the term Δt_a well below 10 fs. The high accelerating fields "freeze" the photo-electron beam zeroing the terms Δt_d and Δt_{sc} .

For an RF deflector, the term Δt_s can be re-written as

$$\Delta t_s = \frac{1}{\pi f V_0 q_e} \frac{m_e c^2}{\sin \Delta \psi} \sqrt{\frac{\gamma \epsilon_n}{\beta_d}}, \quad (2)$$

where c is the speed of light, f is the frequency of the RF deflector, V_0 is the peak deflecting voltage, q_e is the electron

* This project was funded by U.S. Department of Energy under Contract No. DE-AC02-76SF00515.

[†] ftouf@slac.stanford.edu

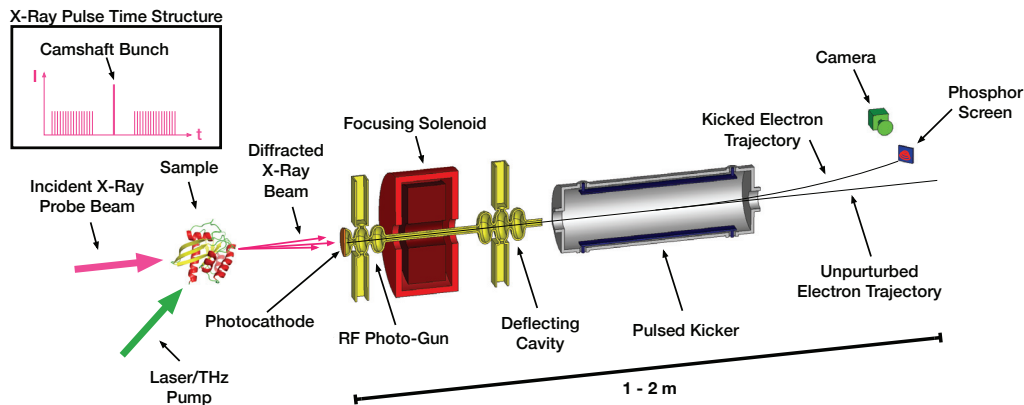
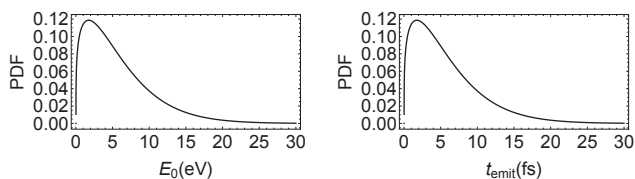


Figure 1: High-Gradient RF Streak Camera Overview.

charge, m_e is the electron rest mass, ϵ_n is the normalized transverse beam emittance, β_d is the beta function at the deflector, and $\Delta\psi$ is the betatron phase advance from the deflector to the screen [27–29]. X-ray beams can be focused on the cathode to 10’s of microns to produce ultra-low emittance electron beams that will be preserved in high-gradient fields. X-Band deflectors have been shown to have a time resolution Δt_s of 1 - 4 fs with low emittance GeV beams in an FEL [29, 30]. Increasing the operating frequency and/or the deflecting gradient could further reduce the term Δt_s , well below 1 fs.



(a) Photon-electron initial energy distribution PDF. (b) Delay of electron emission PDF.

Figure 2: X-ray photoemission model.

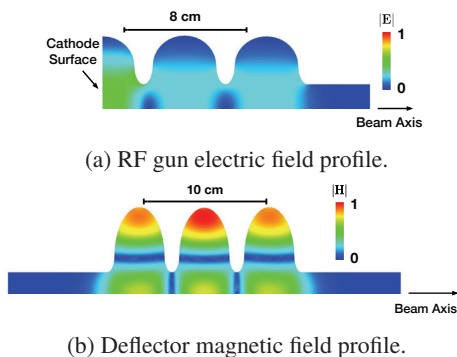


Figure 3: RF structures used in our simulations.

DEVICE CONCEPT

The proposed system is shown in Fig. 1. The X-ray beam hits the photocathode of an RF photo-gun, encoding its tem-

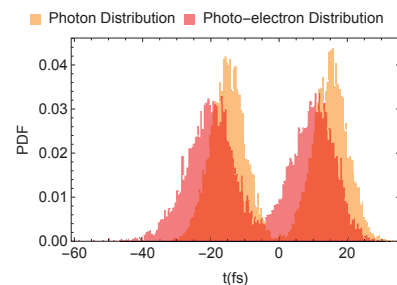
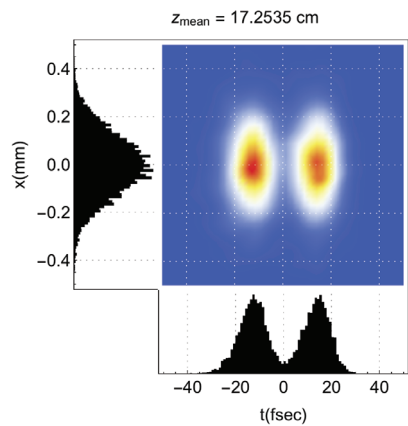


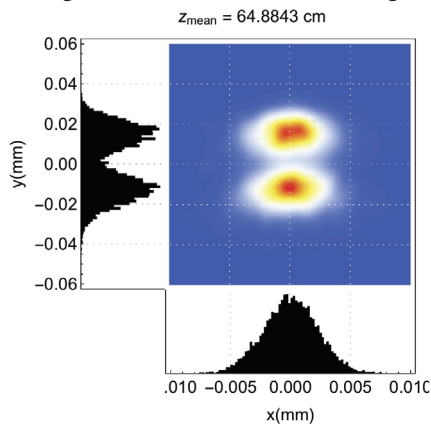
Figure 4: Incident photon versus photo-electron time distributions PDF used in our simulations.

poral and spatial structure into the electron beam. We plan to use a beryllium disk, which acts as a window for the X-rays, coated with gold or other suitable material for photoemission. This cathode is clamped on the photogun copper body. The accelerated electrons are focused with a solenoid and streaked with an RF deflecting cavity. The streaked beam is imaged on a phosphor screen with a high resolution camera.

We are interested in using this system in a synchrotron light source as an ultra-fast camera in order to enable time-resolved pump-probe experiments with long pulses instead of stroboscopy. In this case, the incident X-ray beam hits the sample under investigation and the diffracted photons are imaged on the photocathode. Typically in a storage ring, a special fill pattern is used for pump-probe experiments. The pump is synchronized with a so-called camshaft bunch, which refers to a high-current bunch that is spaced tens of nanoseconds away from all the other low-current bunches. The bunch length in a typical storage ring is relatively long on the order of 20 ps RMS. For this application we can use lower frequency S-Band (2.858 GHz) RF structures with a cycle of 350 ps. Because the filling time of S-Band accelerating structures is large compared to the bunch spacing, the X-rays from all the bunches will be imaged on the photocathode creating parasitic images. In order to solve this problem and isolate the X-ray pulse of the camshaft bunch we will use a fast kicker to direct only the electron bunch generated by the camshaft’s bunch x-rays into the phosphor screen.



(a) Longitudinal distribution after the RF gun.



(b) Transverse beam distribution imaged on a screen after the deflector.

Figure 5: Beam dynamics simulation results.

BEAM DYNAMICS SIMULATION

To generate the initial photo-electron distribution we need the 6D emittance of these electrons. X-ray photoemission between 100 eV and 10 keV has been well studied [24, 31, 32]; however there are virtually no data about the 6D emittance of the photo-electrons. In [24] it is stated that secondary electrons (below 30 eV) comprise 50–90% of the total electrons emitted. The peak energy of the secondary electrons is around 2 eV and the FWHM is below 10 eV. The time spread is on the order of 10 fs. Based on this information we have modeled the initial photo-electron energy distribution and delay between photon absorption and electron emission using a generalized extreme value distribution, as shown in Fig. 2. In this work we ignored the quantum yield and therefore space change.

Figure 3 shows the RF structures we designed for this analysis. We have ignored the RF couplers in this work. The photo-gun has 2.5 cells and the electric field amplitude on the cathode surface is twice the peak on-axis field in the full cells. Its Q_0 is 14,200. For 5 MW of RF power the accelerating gradient on the cathode is 103 MV m^{-1} , the beam energy at the exit is 5 MeV, the peak surface electric and magnetic

fields are 103 MV m^{-1} and 194 kA m^{-1} respectively, and the peak pulsed surface heating [25] for 5 μs pulses is 18°C , well below the copper damage threshold [33]. The deflector has 3 cells. Its Q_0 is 17,600. For 2.5 MW of input power the deflecting voltage is 2.8 MV, the peak surface electric and magnetic fields are 55 MV m^{-1} and 298 kA m^{-1} respectively, and the peak pulsed surface heating [25] for 5 μs pulses is 43°C , which is still considered safe for copper [33].

For injection we have simulated a photon distribution comprised of two 5 fs RMS Gaussian pulses, separated by 30 fs using the beam dynamics simulation code ASTRA [22]. The incident photon beam RMS radius was 50 μm . Fig. 4 shows the photon distribution and resulting photo-electron distribution applying the model of Fig. 2. In ASTRA, the cathode of the RF gun of Fig. 3a was positioned at $z = 0 \text{ m}$ and the center of the deflector of Fig. 3b at $z = 0.5 \text{ m}$. A solenoid was used to focus the beam at the exit of the deflector. Fig. 5a shows the time structure of the electrons at the exit of the gun. The time structure has been well preserved from Fig. 4. Fig. 5b shows the x - y electron distribution at a screen at the exit of the deflector. We can see that the two pulses are clearly distinguished, thus demonstrating the high time resolution of this streak camera.

CONCLUSION

We have presented a new concept for an ultra-fast X-ray streak camera. In this system, the X-ray beam is focused on the photocathode of a high-gradient radio-frequency cavity that accelerates the photo-emitted electrons to a few MeV while preserving their time structure. The accelerated electron beam is streaked by radio-frequency deflectors and then imaged on a phosphor screen. We have shown in beam dynamics simulation that the time resolution of an S-Band device is less than 30 fs, primarily limited by the secondary electron emission time delay.

ACKNOWLEDGEMENTS

The authors wish to thank Georgi Dakovski, Yiping Feng, Ingolf Lindau, Piero Pianetta, Thomas Rabedeau, and Dimosthenis Sokaras for the fruitful conversions.

REFERENCES

- [1] K. Scheidt, "Review of Streak Cameras for Accelerators: Features, Applications and Results," in *Proc. 7th European Particle Accelerator Conf. (EPAC'00)*, Vienna, Austria, Jun. 2000, paper WEYF202, pp. 182–186.
- [2] H. Shiraga, M. Nakasuji, M. Heya, and N. Miyanaga, "Two-dimensional sampling-image x-ray streak camera for ultrafast imaging of inertial confinement fusion plasmas," *Review of Scientific Instruments*, vol. 70, no. 1, pp. 620–623, 1999.
- [3] P. Gallant *et al.*, "Characterization of a subpicosecond x-ray streak camera for ultrashort laser-produced plasmas experiments," *Review of Scientific Instruments*, vol. 71, no. 10, pp. 3627–3633, 2000.
- [4] A. G. MacPhee *et al.*, "Improving the off-axis spatial resolution and dynamic range of the NIF X-ray streak cameras

- (invited),” *Review of Scientific Instruments*, vol. 87, no. 11, p. 11E202, 2016.
- [5] L. Gao *et al.*, “Single-shot compressed ultrafast photography at one hundred billion frames per second,” *Nature*, vol. 516, no. 7529, pp. 74–77, Dec. 2014.
- [6] J. Liang *et al.*, “Encrypted Three-dimensional Dynamic Imaging using Snapshot Time-of-flight Compressed Ultrafast Photography,” *Scientific Reports*, vol. 5, no. 1, p. 15504, Oct. 2015.
- [7] J. Liang *et al.*, “Single-shot real-time video recording of a photonic Mach cone induced by a scattered light pulse,” *Science Advances*, vol. 3, no. 1, p. e1601814, 2017.
- [8] D. S. Badali and R. J. Dwayne Miller, “Robust reconstruction of time-resolved diffraction from ultrafast streak cameras,” *Structural Dynamics*, vol. 4, no. 5, p. 054302, 2017.
- [9] Z. Chang *et al.*, “Demonstration of a sub-picosecond x-ray streak camera,” *Applied Physics Letters*, vol. 69, no. 1, pp. 133–135, 1996.
- [10] J. Liu *et al.*, “An accumulative x-ray streak camera with sub-600-fs temporal resolution and 50-fs timing jitter,” *Applied Physics Letters*, vol. 82, no. 20, pp. 3553–3555, 2003.
- [11] J. Feng *et al.*, “A grazing incidence x-ray streak camera for ultrafast, single-shot measurements,” *Applied Physics Letters*, vol. 96, no. 13, p. 134102, 2010.
- [12] M. M. Shakya and Z. Chang, “Achieving 280fs resolution with a streak camera by reducing the deflection dispersion,” *Applied Physics Letters*, vol. 87, no. 4, p. 041103, 2005.
- [13] J. Feng *et al.*, “An x-ray streak camera with high spatio-temporal resolution,” *Applied Physics Letters*, vol. 91, no. 13, p. 134102, 2007.
- [14] A. Tron and I. Merinov, “Method of bunch radiation photochronography with 10 femtosecond and less resolution,” *International Journal of Modern Physics A*, vol. 22, no. 23, pp. 4187–4197, 2007.
- [15] J. Qiang, J. M. Byrd, J. Feng, and G. Huang, “X-ray streak camera temporal resolution improvement using a longitudinal time-dependent field,” *Nuclear Instruments and Methods in Physics Research Section A: Accelerators, Spectrometers, Detectors and Associated Equipment*, vol. 598, no. 2, pp. 465–469, 2009.
- [16] U. Fröhling *et al.*, “Single-shot terahertz-field-driven X-ray streak camera,” *Nature Photonics*, vol. 3, no. 9, pp. 523–528, Sep. 2009.
- [17] J. Itatani *et al.*, “Attosecond Streak Camera,” *Phys. Rev. Lett.*, vol. 88, p. 173903, Apr. 2002.
- [18] M. Uiberacker *et al.*, “Attosecond metrology with controlled light waveforms,” *Laser Phys.*, vol. 15, pp. 195–204, 2005.
- [19] P. Musumeci *et al.*, “Capturing ultrafast structural evolutions with a single pulse of MeV electrons: Radio frequency streak camera based electron diffraction,” *Journal of Applied Physics*, vol. 108, no. 11, p. 114513, 2010.
- [20] G. H. Kassier *et al.*, “A compact streak camera for 150 fs time resolved measurement of bright pulses in ultrafast electron diffraction,” *Review of Scientific Instruments*, vol. 81, no. 10, p. 105103, 2010.
- [21] C. Lee, G. Kassier, and R. J. D. Miller, “Optical fiber-driven low energy electron gun for ultrafast streak diffraction,” *Applied Physics Letters*, vol. 113, no. 13, p. 133502, 2018.
- [22] K. Floettmann, *ASTRA*, Deutsches Elektronen-Synchrotron, Hamburg, Germany. [Online]. Available: www.desy.de/~mpyflo/Astra_manual/Astra-Manual_V3.1.pdf
- [23] B.-L. Qian and H. E. Elsayed-Ali, “Electron pulse broadening due to space charge effects in a photoelectron gun for electron diffraction and streak camera systems,” *Journal of Applied Physics*, vol. 91, no. 1, pp. 462–468, 2002.
- [24] B. L. Henke, J. A. Smith, and D. T. Attwood, “0.1–10-keV x-ray-induced electron emissions from solids—Models and secondary electron measurements,” *Journal of Applied Physics*, vol. 48, no. 5, pp. 1852–1866, 1977.
- [25] V. A. Dolgashev and S. G. Tantawi, “Effect of RF Parameters on Breakdown Limits in High-Vacuum X-Band Structures,” *AIP Conference Proceedings*, vol. 691, no. 1, pp. 151–165, 2003.
- [26] A. D. Cahill *et al.*, “High gradient experiments with X-band cryogenic copper accelerating cavities,” *Phys. Rev. Accel. Beams*, vol. 21, no. 10, p. 102002, Oct. 2018.
- [27] P. Emma, J. Frisch, and P. Krejcik, “A Transverse RF deflecting structure for bunch length and phase space diagnostics,” Tech. Rep., Aug. 2000.
- [28] R. Akre, L. Bentson, P. Emma, and P. Krejcik, “A Transverse RF deflecting structure for bunch length and phase space diagnostics,” Tech. Rep., Jun. 2001.
- [29] V. A. Dolgashev *et al.*, “Design and application of multi-megawatt X-band deflectors for femtosecond electron beam diagnostics,” *Phys. Rev. ST Accel. Beams*, vol. 17, no. 10, p. 102801, Oct. 2014.
- [30] C. Behrens *et al.*, “Few-femtosecond time-resolved measurements of X-ray free-electron lasers,” *Nature Communications*, vol. 5, p. 336, Apr. 2014.
- [31] B. L. Henke, J. Liesegang, and S. D. Smith, “Soft-x-ray-induced secondary-electron emission from semiconductors and insulators: Models and measurements,” *Phys. Rev. B*, vol. 19, pp. 3004–3021, Mar. 1979.
- [32] B. L. Henke, J. P. Knauer, and K. Premaratne, “The characterization of x-ray photocathodes in the 0.1–10-keV photon energy region,” *Journal of Applied Physics*, vol. 52, no. 3, pp. 1509–1520, 1981.
- [33] L. Laurent, S. Tantawi, V. Dolgashev, C. Nantista, Y. Higashi, M. Aicheler, S. Heikkinen, and W. Wuensch, “Experimental study of rf pulsed heating,” *Phys. Rev. ST Accel. Beams*, vol. 14, no. 4, p. 041001, Apr. 2011.